

Regulation of left-right asymmetry by thresholds of *Pitx2c* activity

Chengyu Liu¹, Wei Liu¹, Mei-Fang Lu¹, Nigel A. Brown² and James F. Martin^{1,*}

¹Alkek Institute of Biosciences and Technology, Texas A&M System Health Science Center, 2121 Holcombe Blvd, Houston, TX 77030, USA

²Department of Anatomy and Developmental Biology, St. George's Hospital Medical School, University of London, Cranmer Terrace, London SW17 0RE, UK

*Author for correspondence (e-mail: jmartin@ibt.tamu.edu)

Accepted 7 March 2001

SUMMARY

Although much progress has been made in understanding the molecular mechanisms regulating left-right asymmetry, the final events of asymmetric organ morphogenesis remain poorly understood. The phenotypes of human heterotaxia syndromes, in which organ morphogenesis is uncoupled, have suggested that the early and late events of left-right asymmetry are separable. The *Pitx2* homeobox gene plays an important role in the final stages of asymmetry. We have used two new *Pitx2* alleles that encode progressively higher levels of *Pitx2c* in the absence of *Pitx2a* and *Pitx2b*, to show that different organs have distinct requirements for *Pitx2c* dosage. The cardiac atria required low *Pitx2c* levels, while the duodenum and lungs used higher *Pitx2c* doses for

normal development. As *Pitx2c* levels were elevated, the duodenum progressed from arrested rotation to randomization, reversal and finally normal morphogenesis. In addition, abnormal duodenal morphogenesis was correlated with bilateral expression of *Pitx2c*. These data reveal an organ-intrinsic mechanism, dependent upon dosage of *Pitx2c*, that governs asymmetric organ morphogenesis. They also provide insight into the molecular events that lead to the discordant organ morphogenesis of heterotaxia.

Key words: Homeobox, Left-right asymmetry, Morphogenesis, Mouse

INTRODUCTION

Current models divide the specification of left-right asymmetry into the initial breaking of symmetry, a secondary phase that propagates an asymmetric signal along the embryo, and the last phase in which each organ interprets the cues that provide an instructive bias for asymmetric morphogenesis (Capdevila et al., 2000; Yost, 1995). It is thought that the biasing signal serves to coordinate asymmetry globally in the embryo. In the absence of bias, as in the *iv* mouse, asymmetric morphogenesis of each organ is uncoupled and randomized (Capdevila et al., 2000). These observations suggest that the local generation of asymmetry within each organ is an all or none, random event (Brown and Wolpert, 1990). The mechanisms that underlie the interaction of the biasing signal with each organ are poorly understood.

Insight into this problem has been obtained by the demonstration that *Pitx2*, a paired-related homeobox gene that was identified as the gene mutated in Rieger syndrome type I (Semina et al., 1996), plays an important role in the local generation of asymmetry within organs. Overexpression studies performed in chick and *Xenopus* embryos suggested that *Pitx2* functioned in handed organs to interpret the asymmetric signals that originate in the pre-somitic embryo (Campione et al., 1999; Logan et al., 1998; Piedra et al., 1998; Ryan et al., 1998). Loss-of-function experiments in mice supported the idea that *Pitx2* played an important role in

asymmetric morphogenesis of multiple organs (Gage et al., 1999; Kitamura et al., 1999; Lin et al., 1999; Lu et al., 1999). However, it remained unclear how a single transcription factor functioned in different contexts to direct both asymmetric organ morphogenesis and the development of symmetric organs such as the teeth and eyes.

Recently, it has been recognized that the *Pitx2* gene encodes three isoforms, *Pitx2a* and *Pitx2b* that are generated by alternative splicing mechanisms, and *Pitx2c* that uses an alternative promoter located upstream of exon 4 (Fig. 1K,L; Kitamura et al., 1999; Schweickert et al., 2000). Although overexpression of any *Pitx2* isoform alters left-right asymmetric organ morphogenesis (Essner et al., 2000; Logan et al., 1998; Ryan et al., 1998), other experiments suggest that *Pitx2a*, *Pitx2b* and *Pitx2c* have distinct expression profiles and target genes (Essner et al., 2000; Kitamura et al., 1999; Schweickert et al., 2000). Thus, different *Pitx2* isoforms may have distinct roles in left-right asymmetry and symmetric organogenesis.

To investigate the function of the *Pitx2* isoforms, we used gene targeting in embryonic stem (ES) cells to generate two new *Pitx2* alleles that deleted *Pitx2a* and *Pitx2b* and encoded varying levels of *Pitx2c*. As the developing heart and lungs express only *Pitx2c*, we used the new *Pitx2* alleles to investigate the requirements for *Pitx2c* in these structures. We also investigated *Pitx2c* function in forming guts, which predominantly express *Pitx2c*. Our data reveal that asymmetric

morphogenesis of the cardiac atria, lungs and duodenum have distinct requirements for *Pitx2c*. Moreover, our results suggest that organ-specific thresholds of *Pitx2c* activity play an important role in asymmetric morphogenesis.

MATERIALS AND METHODS

Gene targeting in ES cells

To generate the targeting vector, we cloned the 5' region of the *Pitx2* gene using PCR amplification. Using intron-spanning oligos in exons 1 and 2, we amplified part of exon 1, the intervening intron and a small region of exon 2 that contains one putative initiator methionine (Arakawa et al., 1998; Gage and Camper, 1997; Semina et al., 1996) from a 129/Sv genomic library. The PCR product was subcloned, sequenced and restriction mapped. The 5' end of the targeting construct, referred to as the δab^{hypoc} targeting vector, was generated from the PCR product, while the 3' end was constructed from a previously characterized *Pitx2* lambda phage clone (Lu et al., 1999). The δab^{hypoc} targeting vector, that contained approximately 6 kb of *Pitx2* homologous sequences, had the IRES *lacZ* cassette cloned into a *Sall* site that was introduced by PCR into the first coding exon of *Pitx2*. After homologous recombination, the δab^{hypoc} allele resulted in deletion of the majority of exon 2 and all of exon 3. In addition, the δab^{hypoc} targeting vector contained the PGKneomycin resistance cassette flanked by LoxP sites that allowed removal of the PGKneomycin to generate the second *Pitx2* allele, the δab allele. The δab^{hypoc} targeting vector was electroporated into AK7 ES cells, targeted clones identified by Southern blot, and injected into 3.5 dpc C57BL/6J mouse embryos to generate chimeras. To induce recombination between the two LoxP sites and remove the PGKneomycin cassette, we crossed δab^{hypoc} chimeras to the CMVCre recombinase deleter strain. The δab^{hypoc} and δab alleles were maintained on a mixed 129/Sv \times C56BL/6J genetic background.

Whole-mount in situ hybridization

Whole-mount in situ hybridization was performed as previously described (Lu et al., 1999). The *Pitx2c*-specific probe was a 1 kb genomic fragment containing exon 4 that was linearized with *Xho*I and transcribed with T7 polymerase. The *Pitx2a* and *Pitx2b*-specific probe was a genomic fragment containing exons 2 and 3 that was linearized with *Not*I and transcribed with T3. The probes for bone morphogenetic protein 4 and sonic hedgehog have been previously described (Echelard et al., 1993; Winnier et al., 1995).

Histology

Embryos were fixed overnight in Bouin's fixative, dehydrated through graded ethanol and embedded in paraffin. Sections were cut at 7 μ m and stained with Hematoxylin and Eosin.

Ribonuclease protection assays

Whole embryo RNA was harvested with triazol reagent (Gibco) according to the manufacturers instructions. Ribonuclease protection assays were performed using the RPA II kit (Ambion). The probe for nuclease protection assays was a *Nco*I/*Not*I subclone from a *Pitx2c* cDNA. *Pitx2c*-protected fragments were quantitated with a phosphoimager and relative values analyzed for statistical significance (ANOVA). Standardization for differences in loading was performed separately using β -actin. Four experiments were performed and the difference in *Pitx2c* levels between $\delta abc^{null} +/-$ and the δabc^{null} , δab^{hypoc} alleles was statistically significant ($P < 0.05$). However, the difference in *Pitx2c* mRNA levels between the $\delta abc^{null} +/-$ and δabc^{null} , δab and between the δabc^{null} , δab^{hypoc} and δabc^{null} ; δab allelic combinations did not reach statistical significance.

RESULTS

Expression of *Pitx2* isoforms

At 8.5 dpc, *Pitx2c* was asymmetrically expressed in left lateral plate mesoderm and left splanchnopleure while *Pitx2a* and *Pitx2b* were expressed only symmetrically in head mesoderm (Fig. 1A,B; Kitamura et al., 1999; Schweickert et al., 2000). At 9.0 dpc, left-sided *Pitx2c* expression persisted in splanchnopleure and forming body wall, while at 10.5 dpc, *Pitx2c* was expressed in left sinus venosus, lung bud and gut (Fig. 1C,D). At these stages, *Pitx2a* and *Pitx2b* were not expressed in forming lung or cardiac structures.

In developing guts, *Pitx2a*, *Pitx2b* and *Pitx2c* were expressed in the stomach, cecal diverticulum, duodenum and midgut (Fig. 1D,F). With the exception of the cecal diverticulum, expression of *Pitx2a* and *Pitx2b* was a minor component of overall *Pitx2* gut expression, and was most readily detectable in mice homozygous for a *Pitx2 lacZ* knock-in allele by X-gal staining (see below and Fig. 1F). *Pitx2c*, *Pitx2a* and *Pitx2b* were expressed symmetrically in oral ectoderm, body wall, umbilical structures and the developing eye at later developmental stages (Fig. 1G,H and not shown).

Isoform-specific deletion of *Pitx2a* and *Pitx2b*

To dissect the functions of the *Pitx2* isoforms, we used gene targeting in ES cells to generate the δab and δab^{hypoc} alleles that removed the *Pitx2a* and *Pitx2b* isoforms by introducing *lacZ* into exon 2 while deleting the coding region of exon 2 and all of exon 3 (Fig. 1K-N). The δab^{hypoc} allele contained a

Fig. 1. Gene targeting and *Pitx2* isoform expression. (A,B) 8.5 dpc expression of *Pitx2c* (A), *Pitx2a* and *Pitx2b* (B). Arrow denotes sinus venosus and arrowhead indicates lateral mesoderm. (C) 9.0 dpc expression of *Pitx2c*. bw, body wall; sp, splanchnopleure. (D,E) 10.5 dpc expression of *Pitx2c* in wild-type (D) and δab ; δab^{hypoc} embryos (E). lb, lung bud; s, stomach. (F) X-gal staining in δab ; δab^{hypoc} guts. c, cecal diverticulum; d, duodenum; mg, midgut; sma, superior mesenteric artery. (G,H) 10.5 dpc expression of *Pitx2c* (G), *Pitx2a* and *Pitx2b* (H). oe, oral ectoderm; pm, pericardial mesenchyme. (I,J) Eye phenotypes (arrowhead) of wild-type (I) and δab ; δab^{hypoc} (J) embryos. (K) Exon usage of *Pitx2* isoforms. (L) *Pitx2* genomic structure and targeting strategy. The boxes represent exons and straight lines introns. The exons are not drawn to scale. (M) Targeted allele before and after removal of the PGKneomycin cassette. At the bottom is the *Pitx2*-null allele that was previously generated (Lu et al., 1999). (N) Southern blot with flanking probes: tail DNA probed with the 5' flanking probe (left); tail DNA probed with the 3' flanking probe (center). The right panel shows a Southern blot probed with an internal *lacZ* probe after crossing the $\delta ab^{hypoc} +/-$ mice to the CMV cre recombinase deleter strain to generate $\delta ab +/-$ mice. After recombination, and PGKneomycin removal, the *lacZ* probe hybridizes to a 2 kb fragment, while in mice that still retain the PGKneomycin, the *lacZ* probe hybridizes to a 3 kb fragment. In the right-hand panel, + above the lanes denotes mice that have retained PGKneomycin and - denotes a mouse that has deleted PGKneomycin. (O) Diagram of riboprobe that distinguishes between isoforms and the *Pitx2c*-protected fragment. (P) Ribonuclease protection assay of mRNA from *Pitx2* allelic combinations: 1, probe; 2,3, tRNA; 4,5, wild type; 6, δabc^{null} heterozygous; 7,8, δabc^{null} ; δab ; 9,10, δabc^{null} ; δab^{hypoc} ; 11,12, δabc^{null} ; δabc^{null} ; 13, markers. (Q) Quantitation of *Pitx2c* mRNA levels in the different *Pitx2* allelic combinations.

LoxP-flanked PGKneomycin cassette that was removed with Cre recombinase to create the δab allele (Fig. 1M,N). We intercrossed $\delta ab^{+/-}$ mice and found that a proportion of

$\delta ab; \delta ab$ mice were viable and fertile. Genotyping of weanling progeny from crosses between $\delta ab; \delta ab$ and $\delta ab^{+/-}$ mice showed that 29% were homozygous mutant, suggesting a loss

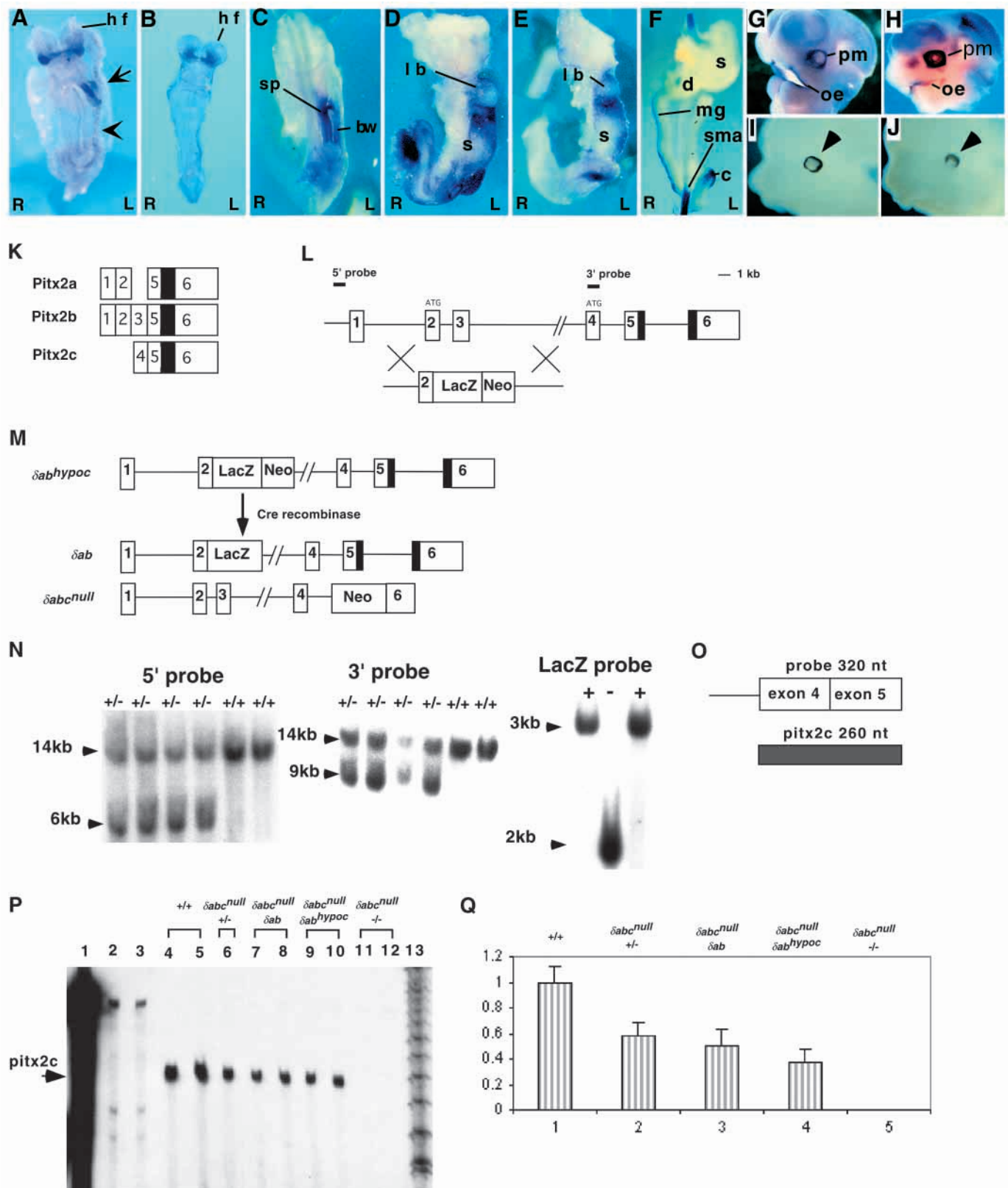


Fig. 1

(21%) of homozygous mutant mice in the postnatal period ($n=58$). Analysis of neonatal $\delta ab; \delta ab$ mice revealed that postnatal lethality was secondary to cleft palate (9%; $n=30$) or midgut malrotation (87%; $n=30$) that in some cases resulted in volvulus and bowel infarction. In addition, we found that $\delta ab; \delta ab$ mutants had eye defects (Fig. 1I,J).

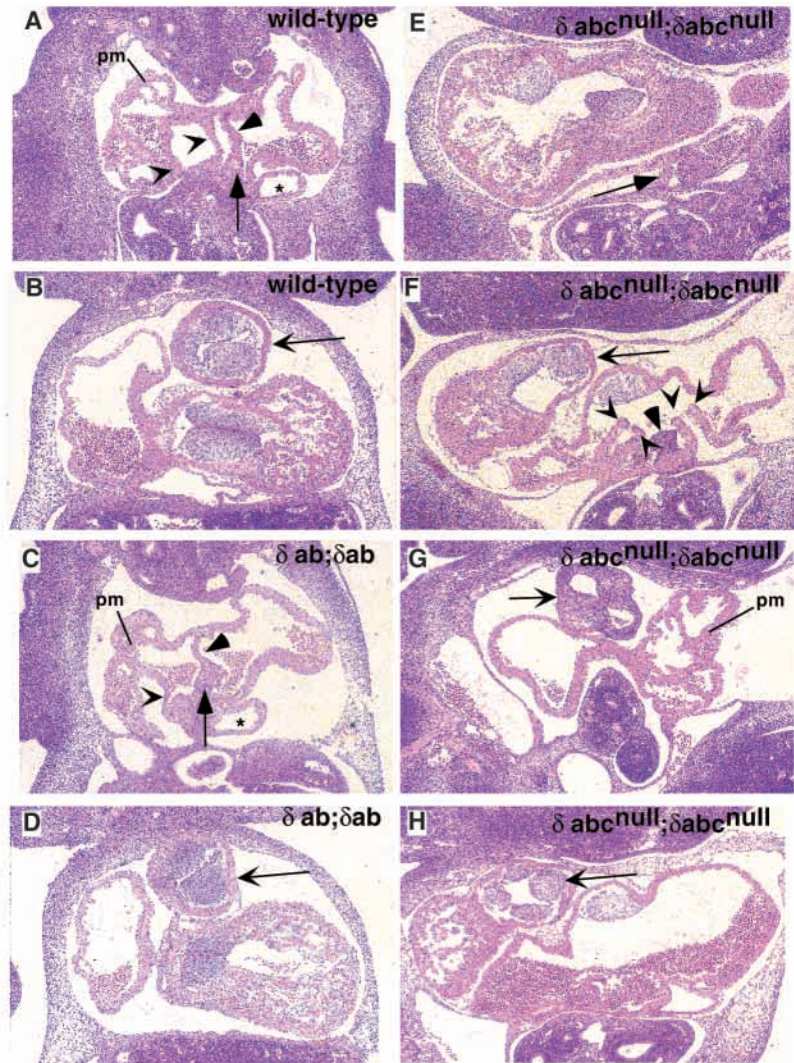
We examined the expression pattern of *Pitx2c* in 10.5 dpc $\delta ab; \delta ab$ mutant embryos. *Pitx2c* expression in left lung bud and left gut in $\delta ab; \delta ab$ mutants was identical to wild-type littermate controls (Fig. 1D,E) suggesting that spatial expression of *Pitx2c* from the δab allele is similar to the wild-type allele. We also performed ribonuclease protection assays on whole 12.5 dpc embryo mRNA using a probe that distinguishes between *Pitx2* isoforms (Fig. 1O,P) to measure *Pitx2c* levels in δabc^{null} heterozygotes and $\delta abc^{null}; \delta ab$ and $\delta abc^{null}; \delta ab^{hypoc}$ allelic combinations. As the δabc^{null} allele does not express *Pitx2c* (Fig. 1P, lanes 11 and 12; Fig. 1Q, lane 5), this analysis measured *Pitx2c* expression from the wild-type, the δab and the δab^{hypoc} alleles.

We found that expression of *Pitx2c* in the δabc^{null} heterozygotes was $58 \pm 11\%$ compared with embryos with two wild-type *Pitx2* alleles (Fig. 1P, lane 6; Fig. 1Q, compare lanes 1 and 2). Expression of *Pitx2c* in the $\delta abc^{null}; \delta ab$ embryos was $50 \pm 14\%$ (not statistically significant when compared with $\delta abc^{null} +/-$; Fig. 1P lanes 7,8; Fig. 1Q compare lanes 2 and 3); in the $\delta abc^{null}; \delta ab^{hypoc}$ embryos, *Pitx2c* expression was $37 \pm 11\%$ ($P < 0.05$, compared with $\delta abc^{null} +/-$; Fig. 1P, lanes 9,10; Fig. 1Q compare lanes 2 and 4). These results show that the δab^{hypoc} allele encodes significantly reduced levels of *Pitx2c* mRNA compared with the wild-type allele in the δabc^{null} heterozygous embryos. Moreover, the ribonuclease protection assay data suggest a trend in which the δab allele encodes levels of *Pitx2c* intermediate between that of the δab^{hypoc} and wild-type alleles.

The δab^{hypoc} and δab alleles encode different degrees of *Pitx2c* function

Although the ribonuclease protection assay analysis suggests that *Pitx2c* levels are comparable in the δab^{hypoc} and δab alleles, it is possible that this analysis has missed subtle, but biologically significant differences between the two alleles. Moreover, as it has been reported that a retained PGKneomycin cassette in an intron can interfere with *Pitx2* function (Gage et al., 1999), we suspect that the PGKneomycin in the δab^{hypoc} locus might also have a deleterious effect on *Pitx2c* function.

In order to test this idea and determine if the δab^{hypoc} and δab alleles encode equivalent *Pitx2c* function, we performed a genetic experiment and intercrossed these *Pitx2* alleles with the δabc^{null} allele. The $\delta abc^{null}; \delta abc^{null}$ mutant embryos, that lack all *Pitx2* function, died by 14.5 dpc (Gage et al., 1999; Kitamura et al., 1999; Lin et al., 1999; Lu et al., 1999). In contrast, intercrosses between the δabc^{null} and δab^{hypoc} heterozygous mice showed that about half of $\delta abc^{null}; \delta ab^{hypoc}$ embryos were still alive at 16.5 dpc (Table 1). Moreover, the



$\delta abc^{null}; \delta ab$ mutants survived 2 days longer, as embryo loss was first detected at 18.5 dpc (Table 2). These genetic data suggest that the $\delta abc^{null}; \delta ab^{hypoc}$ and $\delta abc^{null}; \delta ab$ embryos survive longer than $\delta abc^{null}; \delta abc^{null}$ embryos because of residual *Pitx2c* function. In addition, as a result of the retained

Table 1. Embryo recovery: $\delta abc^{null} +/- \times \delta ab^{hypoc} +/-$ intercrosses

| Stage | +/+ | $\delta abc^{null} +/-$ | $\delta ab^{hypoc} +/-$ | $\delta abc^{null}/\delta ab^{hypoc}$ | Mutant/total (%) |
|-------|-----|-------------------------|-------------------------|---------------------------------------|------------------|
| 10.5 | 12 | 12 | 20 | 18 | 18/62 (29) |
| 12.5 | 19 | 25 | 26 | 28 | 28/98 (28) |
| 14.5 | 4 | 8 | 9 | 3 | 3/24 (13) |
| 16.5 | 11 | 5 | 6 | 3 | 3/25 (12) |

Table 2. Embryo recovery from $\delta abc^{null} +/- \times \delta ab -/-$ intercrosses

| Stage | $\delta ab +/-$ | $\delta abc^{null}; \delta ab$ | Mutant/total (%) |
|-------|-----------------|--------------------------------|------------------|
| 10.5 | 9 | 8 | 8/17 (47) |
| 12.5 | 28 | 30 | 30/58 (52) |
| 16.5 | 15 | 14 | 14/29 (48) |
| 18.5 | 11 | 3 | 3/14 (21) |

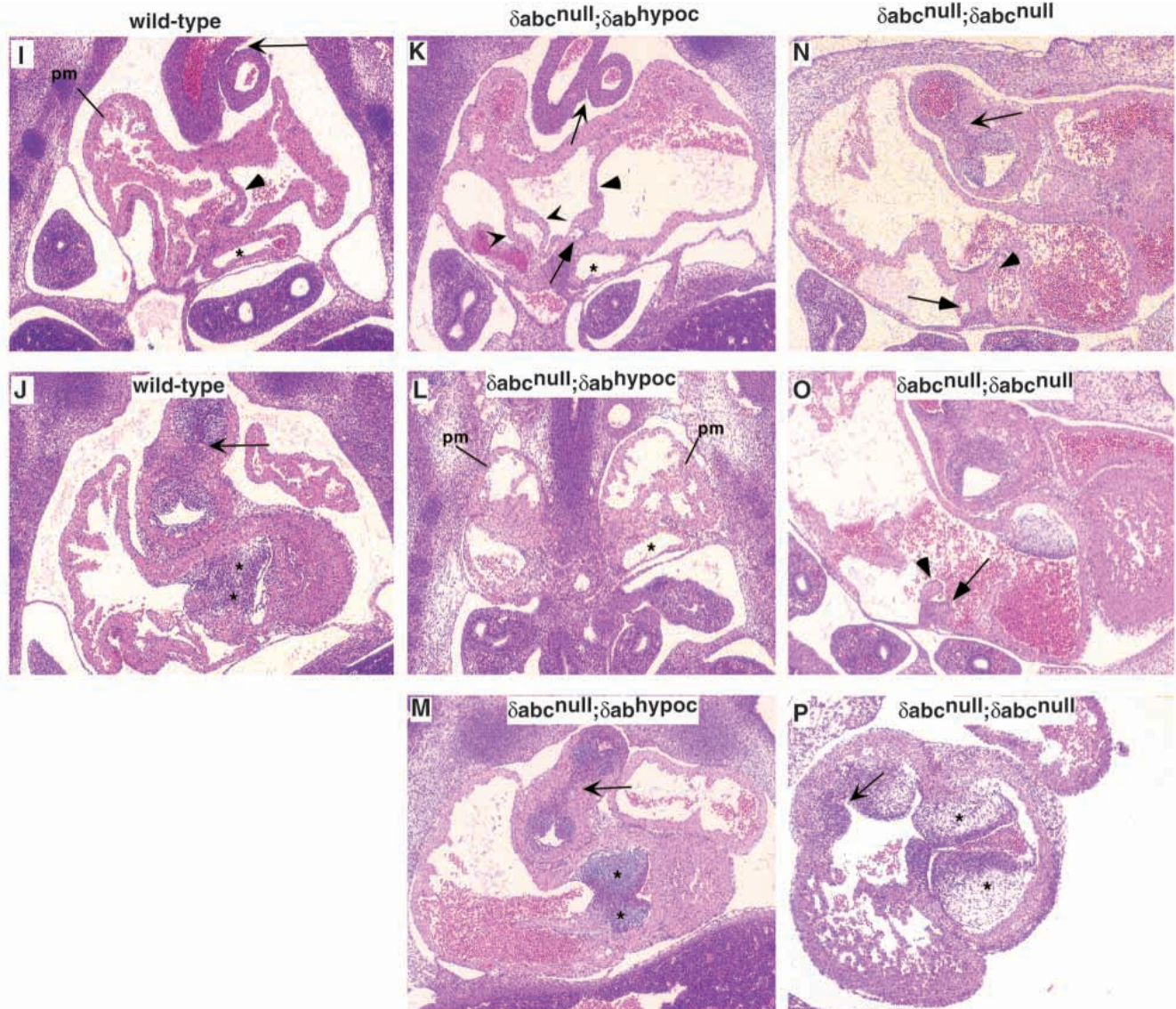


Fig. 2. Cardiac phenotypes of *Pitx2* allelic combinations. (A-D) Transverse sections through 11.5 dpc hearts of wild-type and $\delta ab; \delta ab$ mutants. In wild-type (+;+) and $\delta ab; \delta ab$ embryos, the primary interatrial septum (PIAS) extends from the spina vestibuli to the roof of the atrium (solid arrowheads, A,C) and the pulmonary vein is located at the base of the PIAS (blunt arrow in A,C). Paired venous valves are found at the boundary of the right atrium and right sinus horn (winged arrowheads in A,C). In wild-type and $\delta ab; \delta ab$ hearts, the cushions of the proximal OFT occlude the lumen, and twist in characteristic fashion, with left and right lateral lumens (arrows in B,D). Moreover, the right side of the atrium has trabeculations (pectinate muscles, pm in A and C), while the left side has none. (E-H) Transverse sections through 11.5 dpc $\delta abc^{null}; \delta abc^{null}$ hearts. In $\delta abc^{null}; \delta abc^{null}$ mutant embryos, the PIAS is just a stub (blunt arrowhead in F) and the pulmonary vein has an anomalous connection, emptying into the right sinus horn, or saccus reuniens (arrow, E). Also in $\delta abc^{null}; \delta abc^{null}$ mutant embryos, paired venous valves are present on both the left and right (winged arrowheads in F). The mutant OFT has a large lumen with symmetrical cushions (winged arrows in F-H) and the dorsal left atrium is more extensively trabeculated than the right (pm in G). The left superior caval vein, present in wild-type and $\delta ab; \delta ab$ hearts (asterisks in A and C), is absent in $\delta abc^{null}; \delta abc^{null}$ hearts. (I-M) Transverse sections through 12.5 dpc hearts of wild-type and $\delta abc^{null}; \delta ab^{hypoc}$ mutants. The PIAS is normal (blunt arrowheads I and K) and the pulmonary vein is located at base of PIAS (blunt arrow K) in wild-type and $\delta abc^{null}; \delta ab^{hypoc}$ embryos. The distal OFT is separated into the left aortic arch and the right pulmonary trunk (winged arrows in I and K) and the proximal OFT cushions form three primordia of valve leaflets in both arterial trunks, although septation is incomplete (winged arrows, J,M). The right atrium in wild-type hearts has trabeculations (pm, I), while the left atrium has none. The dorsal left and right atria of $\delta abc^{null}; \delta ab^{hypoc}$ hearts have similar degrees of trabeculation (pm, L). The superior and inferior AV cushions have fused in wild-type and $\delta abc^{null}; \delta ab^{hypoc}$ hearts (asterisks, J,M), forming separate left and right AV canals. (N-P) Transverse sections through 12.5 dpc $\delta abc^{null}; \delta abc^{null}$ hearts. In $\delta abc^{null}; \delta abc^{null}$ mutants, the PIAS is truncated (blunt arrowheads, O) and the pulmonary vein is found within dorsal mesocardium, but caudal to the atrial wall, so emptying into the right sinus horn, or saccus reuniens (blunt arrow, N). The pulmonary vein has exits to both the left side (blunt arrow, O) and the right side (not shown) in $\delta abc^{null}; \delta abc^{null}$ embryos. The $\delta abc^{null}; \delta abc^{null}$ mutant distal OFT is unseptated, with malaligned arterial trunks (winged arrow, N) and the OFT cushions are malaligned (winged arrow, P). Moreover, the AV cushions have not fused, and there is a common AV junction (asterisk, P) in $\delta abc^{null}; \delta abc^{null}$ embryos. The left superior caval vein shown in wild-type and $\delta abc^{null}; \delta ab^{hypoc}$ hearts (asterisks in I,K,L) is absent in $\delta abc^{null}; \delta abc^{null}$ hearts.

PGKneomycin cassette, the δab^{hypoc} allele encodes less Pitx2c function than the δab allele. Other genetic evidence, obtained from analysis of lung phenotypes, also suggests that the δab allele encodes slightly less Pitx2c than the wild-type allele (see below).

We used the δab and δab^{hypoc} alleles, in conjunction with the wild-type and δabc^{null} alleles, to generate *Pitx2* allelic combinations that encode varying levels of Pitx2c, in order to investigate the dose requirements for Pitx2c in asymmetric morphogenesis.

Pitx2c provides left identity to atrial primordia

Although $\delta abc^{null}; \delta abc^{null}$ mutant mice have correct rightward ventricular looping, they have numerous defects in cardiac development (Gage et al., 1999; Kitamura et al., 1999; Lin et al., 1999; Lu et al., 1999). Normal right atrial structures include the coronary sinus and the venous valves, while the left atrium has the pulmonary vein. Histological analysis showed that $\delta abc^{null}; \delta abc^{null}$ mutants had no coronary sinus, bilateral venous valves, anomalous pulmonary venous drainage, and a deficiency in the primary interatrial septum (compare Fig. 2A,B,I with 2E-H,N,O). The outflow tract cushions of $\delta abc^{null}; \delta abc^{null}$ mutants were symmetric and the trunks of the great arteries were malaligned and unseptated (compare Fig. 2B with 2G,H,N,P). In addition, all had defects in ventriculoarterial connections, usually double outlet right ventricle (DORV), and some had a common atrioventricular canal (Fig. 2J,P). This spectrum of morphological defects is specifically associated with right isomerism in human hearts (Brown and Anderson, 1999), and strongly suggests that the $\delta abc^{null}; \delta abc^{null}$ embryos had right atrial isomerism.

All these cardiac defects were completely rescued in $\delta abc^{null}; \delta ab^{hypoc}$, $\delta abc^{null}; \delta ab$ allelic combinations and in $\delta ab; \delta ab$ mutant embryos (compare Fig. 2A,B,I,J with 2C,D,K,M). This suggests that Pitx2c is the important *Pitx2* isoform for most of cardiac morphogenesis, and that only

low Pitx2c levels are required. An invariable distinguishing feature between the formed left and right atrium is the morphology of the pectinate muscles (Brown and Anderson, 1999; Uemura et al., 1995). On the right hand side, the pectinate muscles are extensive and encircle the vestibule, while in the left atrium pectinate muscles are fewer and confined within the appendage. At embryonic stages, this is reflected in the degree of atrial trabeculation, with more in the right than left (Fig. 2A,I). In $\delta abc^{null}; \delta abc^{null}$ mutant embryos, the pattern of pectinate trabeculation was reversed, being more extensive on the left than the right (Fig. 2G). As the dose of Pitx2c was increased in *Pitx2* allelic combinations, pectinate trabeculation pattern was rescued. In $\delta abc^{null}; \delta ab^{hypoc}$ and $\delta abc^{null}; \delta ab$ embryos, there was approximately the same amount of trabeculation in right and left atria (Fig. 2L), while in $\delta ab; \delta ab$, the pattern was apparently normal (Fig. 2C). Thus, low levels of Pitx2c are sufficient for the development of most of the atrium, but higher levels are required for left identity of the atrial appendages.

Requirement for Pitx2c, Pitx2a and Pitx2b in lungs

Primary lung buds and mature lungs, which develop as an outpouching of the foregut, have left-right asymmetric morphology (Hogan, 1999; Fig. 3A,B). It has previously been shown that $\delta abc^{null}; \delta abc^{null}$ embryos have complete right pulmonary isomerism (Gage et al., 1999; Kitamura et al., 1999;

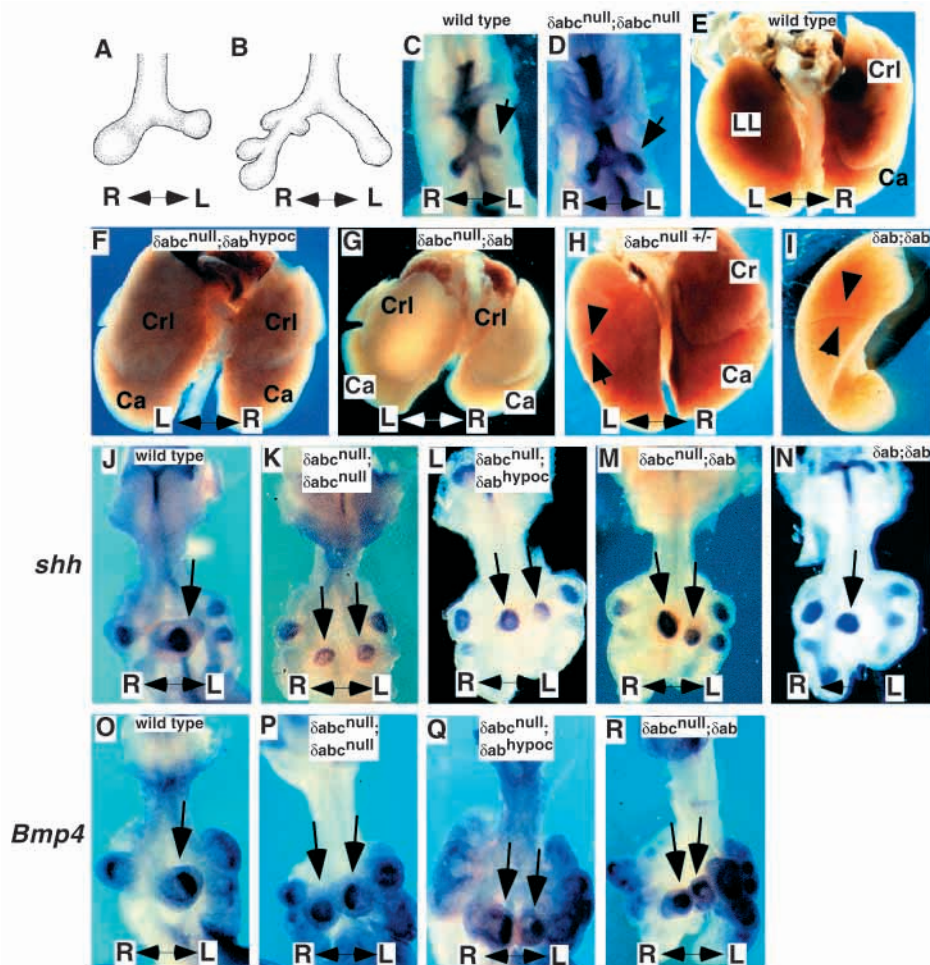


Fig. 3. Lung phenotypes of *Pitx2* allelic combinations. (A,B) Diagram of asymmetric lung branching pattern. (C,D) Whole-mount in situ hybridization with the sonic hedgehog probe in 9.0 dpc wild-type (C) and $\delta abc^{null}; \delta abc^{null}$ (D) embryos. (E-I) Dorsal aspect of adult wild-type (E), neonatal $\delta abc^{null}; \delta ab^{hypoc}$ (F), $\delta abc^{null}; \delta ab$ (G), $\delta abc^{null} +/-$ (H) or oblique view of $\delta ab; \delta ab$ (I). Ca, caudal lobe; CrI, cranial lobe; LL, left lung. (J-N) 11.5 dpc whole-mount in situ with probe for sonic hedgehog: wild-type (J), $\delta abc^{null}; \delta abc^{null}$ (K), $\delta abc^{null}; \delta ab^{hypoc}$ (L), $\delta abc^{null}; \delta ab$ (M) and $\delta ab; \delta ab$ (N). (O-R) 12.0 dpc whole-mount in situ with probe for bone morphogenetic protein 4: wild-type (O), $\delta abc^{null}; \delta abc^{null}$ (P), $\delta abc^{null}; \delta ab^{hypoc}$ (Q) and $\delta abc^{null}; \delta ab$ (R).

Lin et al., 1999; Lu et al., 1999). Consistent with the expression of Pitx2c in left splanchnopleure and primary lung buds, we found that pulmonary right isomerization was evident at the primary lung bud stage in $\delta abc^{null}; \delta abc^{null}$ embryos (Fig. 3C,D).

We found evidence for right isomerism in all *Pitx2* allelic combinations. The lungs of $\delta abc^{null}; \delta ab^{hypoc}$ and $\delta abc^{null}; \delta ab$ neonates showed nearly complete right pulmonary isomerism (Fig. 3E-G), suggesting that pulmonary morphogenesis is very sensitive to diminished Pitx2c function. We also found that 25% ($n=16$) of δabc^{null} heterozygous adults had partial right lung isomerization in which an extra fissure developed at the cranial aspect of the left lung (Fig. 3H). Moreover, 83% of $\delta ab; \delta ab$ neonates revealed an extra fissure between what would be the cranial and middle lobes (Fig. 3I), suggesting a minor role for Pitx2a and Pitx2b in pulmonary morphogenesis. Consistent with this notion, Pitx2a and Pitx2b expression has been detected in adult lung tissue (Gage and Camper, 1997). The mild lung phenotype of the δabc^{null} heterozygotes, containing one copy of Pitx2c and one copy of Pitx2a and Pitx2b, compared with the severe lung phenotype of $\delta abc^{null}; \delta ab$

mutants, which have one copy of Pitx2c but no Pitx2a and Pitx2b, suggests that the δab allele encodes less Pitx2c function than the wild-type allele.

We investigated the secondary lung bud branching pattern in *Pitx2* allelic combinations using whole-mount in situ hybridization with probes for sonic hedgehog (Shh), which marks lung bud endoderm, and bone morphogenetic protein 4 (Bmp4), which marks both endoderm and mesoderm (Bellusci et al., 1996; Bellusci et al., 1997). In $\delta abc^{null}; \delta abc^{null}$ mutant embryos, the left-sided branching pattern was identical to that of the right lung bud or right isomerized (Fig. 3J,K,O,P). In both $\delta abc^{null}; \delta ab^{hypoc}$ and $\delta abc^{null}; \delta ab$ embryos, the left-sided branching pattern was also right isomerized (Fig. 3L,M,Q,R). This suggested that these *Pitx2* allelic combinations fail to express adequate Pitx2c for normal left-sided branching morphogenesis. The initial aspects of branching morphogenesis in $\delta ab; \delta ab$ mutant embryos were similar to wild-type, suggesting a later, minor function for Pitx2a and Pitx2b in pulmonary morphogenesis (Fig. 3N). Based on these phenotypes, and the expression pattern of Pitx2c in left splanchnic mesoderm and left primary lung bud,

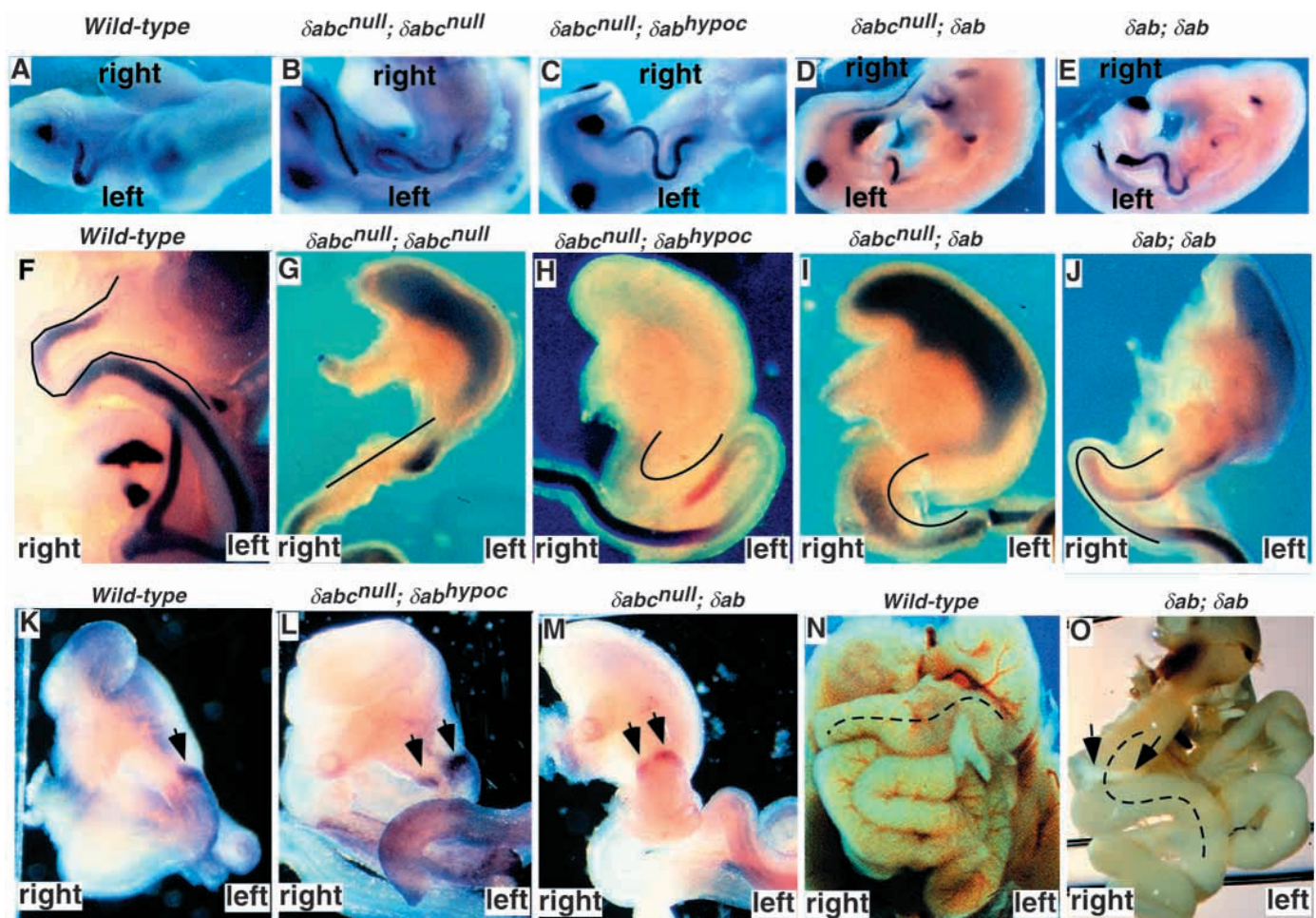


Fig. 4. Gut phenotypes of *Pitx2* allelic combinations. (A-E) Gut looping in 10.5 dpc embryos visualized using the probe for sonic hedgehog. Genotypes are shown. (F-J) Duodenal rotation in 12.5 dpc embryos visualized using the probe for sonic hedgehog. Genotypes are shown. Direction of duodenal rotation is outlined. (K-M) *Pitx2c* expression in duodenum shown by whole-mount in situ hybridization. Note bilateral expression as denoted by the arrows. (N,O) Normal and arrested midgut rotation in wild-type (N) and $\delta ab; \delta ab$ mutant (O) embryos. Direction of midgut looping is outlined. Annular pancreas in $\delta ab; \delta ab$ mutant embryo (O) is denoted by arrows.

Table 3. Duodenal rotation phenotypes of *Pitx2* allelic combinations

| Genotype | Arrest number (%) | Reversed number (%) | Correct number (%) |
|--|-------------------|---------------------|--------------------|
| $\delta abc^{null} -/-$ | 13/18 (72) | 3/18 (17) | 2/18 (11) |
| $\delta abc^{null}; \delta ab^{hypoc}$ | 2/14 (14) | 5/14 (36) | 7/14 (50) |
| $\delta abc^{null}; \delta ab$ | 0/18 (0) | 15/18 (83) | 3/18 (17) |
| $\delta ab -/-$ | 0/32 (0) | 4/32 (12.5) | 28/32 (88) |
| $\delta abc^{null} +/-$ | 0/67 (0) | 0/67 (0) | 67/67 (100) |

we conclude that high levels of *Pitx2c* in the lung primordia are necessary for left-specific lung morphogenesis.

***Pitx2c* cooperates with *Pitx2a* and *Pitx2b* to regulate gut morphogenesis**

The duodenum, the most rostral part of the small intestine, forms from distal foregut and rostral midgut. The early gut tube loops to the left, then as the duodenum develops, it rotates to the right to form a C-shaped structure with stereotypical relationships to the liver, pancreas and biliary tree (Moore, 1982). In all *Pitx2* allelic combinations, the initial bending of the gut tube to the left was unaffected (Fig. 4A-E). However, in $\delta abc^{null}; \delta abc^{null}$ embryos, rotation of the duodenum failed to occur in the majority (72%, $n=18$) of embryos examined (Fig. 4F,G). A small percentage had correct or reversed rotation at the duodenum (Table 3).

As the dosage of *Pitx2c* was increased in *Pitx2* allelic combinations that had no *Pitx2a* and *Pitx2b*, duodenal rotation was rescued; however, orientation was initially randomized and then reversed. In $\delta abc^{null}; \delta ab^{hypoc}$ embryos, which have the lowest levels of residual *Pitx2c*, one half of embryos had correctly oriented duodenal rotation, while 36% had reversed rotation and 14% failed to rotate (Fig. 4H; Table 3). In contrast, the majority (83%) of $\delta abc^{null}; \delta ab$ embryos showed reversal of duodenal rotation (Fig. 4I; Table 3). Therefore, as *Pitx2c* levels gradually increased, duodenal rotation became fixed in a reverse orientation. Finally, most (88%; $n=30$) of $\delta ab; \delta ab$ neonates and all of δabc^{null} heterozygotes had correct rotation of the duodenum (Fig. 4J and Table 3), showing that at these doses of *Pitx2c* the duodenum developed correctly.

We examined duodenal *Pitx2c* expression, that is normally left-sided, in $\delta abc^{null}; \delta ab$ and $\delta abc^{null}; \delta ab^{hypoc}$ embryos. *Pitx2c* was bilaterally expressed in the duodenum of these mutant embryos, suggesting the existence of a regulatory mechanism within the developing gut that normally restricts *Pitx2c* expression to the left side (Fig. 4K-M).

As midgut develops, it forms a cranial limb that gives rise to small bowel and a caudal limb that develops into large intestine. The midgut limbs rotate through a 270° counterclockwise movement that results in the final positioning of the small and large bowels (Moore, 1982). In 87% ($n=30$) of $\delta ab; \delta ab$ neonates, the midgut failed to rotate resulting in a right-sided midgut mass (Fig. 4N,O). In the remainder ($n=4$) of $\delta ab; \delta ab$ neonates midgut rotation arrested midway through rotation. In addition, 21% of $\delta ab; \delta ab$ neonates showed annular pancreas (Fig. 4O).

DISCUSSION

We have used isoform-specific deletions of *Pitx2a* and *Pitx2b*

that encode varying levels of *Pitx2c* to investigate *Pitx2c* function during left-right asymmetry. Our data reveal an organ-intrinsic mechanism based on differential response to *Pitx2c* dose for regulating asymmetric morphogenesis. Our results provide insight into the normal mechanisms regulating left-right asymmetric morphogenesis in which different developmental fields have varying requirements for *Pitx2c* levels.

Cardiac development requires only low *Pitx2c* levels

The cardiac atria were right isomerized in $\delta abc^{null}; \delta abc^{null}$ mutant embryos. We found right sino-atrial isomerism, including symmetry of sinus horns and bilateral paired venous valves, and abnormalities of atrioventricular and ventriculoarterial connections. In contrast, $\delta abc^{null}; \delta ab^{hypoc}$ and $\delta abc^{null}; \delta ab$ embryos, which encode the next highest levels of *Pitx2c*, had almost normal atria. From these data, we conclude that only low levels of *Pitx2c* are necessary to provide left identity to most of the atrium. These results also provide insight into the observation that cardiac anomalies, although described in families with Rieger syndrome, are uncommon (Bekir and Gungor, 2000; Cunningham et al., 1998; Mammi et al., 1998). In contrast, the atrial pectinate pattern requires higher levels of *Pitx2c*. In this respect, the atrial appendages resemble the lungs, although higher *Pitx2c* levels are required by the lung primordia. This fits well with the clinical observation that isomeric atrial appendages are virtually always associated with isomeric lung lobation (Brown and Anderson, 1999). In addition, the lung and atrial appendage primordia develop in close proximity.

Lungs need the highest doses of *Pitx2c*

Forming lungs require high levels of *Pitx2c* for normal morphogenesis. The $\delta abc^{null}; \delta ab^{hypoc}$ and $\delta abc^{null}; \delta ab$ allelic combinations, which had nearly normal hearts, showed strong right pulmonary isomerism phenotypes. Branching morphogenesis involves a reiterative branching mechanism in which an initial pattern is established and modified at successive steps in a stereotypical fashion (Hogan, 1999; Metzger and Krasnow, 1999). Our finding that the primary lung buds of $\delta abc^{null}; \delta abc^{null}$ mice are right isomerized suggests that *Pitx2c* functions prior to or at the initial stages of the branching process. The lung phenotypes of the $\delta ab; \delta ab$ mutants suggest that *Pitx2a* and *Pitx2b* has a later, more restricted function in lung morphogenesis.

Tight control of *Pitx2c* in duodenal organogenesis

The progression of duodenal phenotypes with increasing *Pitx2c* dosage revealed an organ-intrinsic mechanism to distinguish between randomization and reversal. The biasing model of asymmetric organ morphogenesis suggests that absence of biasing would result in organ randomization, as in the *iv;iv* mouse (Brown and Wolpert, 1990; Capdevila et al., 2000). Our data suggest that an intermediate level of biasing can result in reversed organ morphogenesis.

Bilateral duodenal *Pitx2c* expression in $\delta abc^{null}; \delta ab^{hypoc}$ and $\delta abc^{null}; \delta ab$ embryos suggests a mechanism within the duodenum that inhibits right-sided *Pitx2c* expression. This raises the possibility that relative left- versus right-sided *Pitx2c* levels determine the direction of gut rotation. In support of this idea, studies in *Xenopus* have shown that overexpression of

Pitx2 on the left or right resulted in defective asymmetric morphogenesis (Essner et al., 2000). Moreover, these studies also showed that gut development was more susceptible to right-sided misexpression of *Pitx2* than the heart (Essner et al., 2000), further supporting the notion of organ-specific requirements for *Pitx2* function.

Our data also demonstrate that different regions of the gut are regulated by distinct mechanisms. Duodenal morphogenesis was most sensitive to changes in *Pitx2c* levels, while morphogenesis of the stomach was unaffected. In addition, midgut development appears to be regulated by the *Pitx2a* and *Pitx2b* isoforms, although it is possible that very high levels of *Pitx2c* are required for midgut development and that a slight decrease in *Pitx2c* expression from the δab allele is sufficient to disrupt midgut looping. Overexpression studies performed in *Xenopus* have also demonstrated that regional gut asymmetry can be unlinked (Bisgrove et al., 2000).

An organ-specific response to biasing

Current models propose that a biasing signal, originating at the node in mice, provides a cue that each organ uses to initiate correctly oriented asymmetric morphogenesis (Brown and Wolpert, 1990; Capdevila et al., 2000). The implication of these ideas is that asymmetric morphogenesis is all or none, either reversed or correct morphogenesis. Isomerism or loss of asymmetry would result from defects in interpretation of biasing at the organ level. Under this paradigm, uncoupling of asymmetry would be a result of defective biasing. This is illustrated by the *iv* and *lefty1* mouse mutants that show heterotaxy (Brown and Anderson, 1999; Brown et al., 1989; Meno et al., 1998; Supp et al., 1997), implicating events occurring during the initial breaking of symmetry (*iv* mice) and the stabilization of left-sided gene expression by a midline barrier (*lefty1* mice) in the etiology of heterotaxia. In contrast, our data suggest that left-right asymmetry within each organ is regulated not as an all-or-none decision but rather in stages. Thus, defects at the organ level, acting after biasing, can also result in heterotaxia.

Concluding remarks

We have shown that a central component of the local generation of asymmetry within an organ is a differential response to *Pitx2c*. These different requirements for *Pitx2c* dose may reflect the different morphogenetic processes, ranging from rotation of a tube to reiterated budding morphogenesis, that occur during asymmetric morphogenesis. It is conceivable that *Pitx2c* regulates different target genes in each organ. For example, in the atrium, *Pitx2c* may regulate target genes with high-affinity binding sites, while in the lung, *Pitx2c* target genes would have low-affinity regulatory elements. This model has the advantage of providing an understanding for how *Pitx2c* may regulate different morphogenetic events. Alternatively, there may exist organ-specific mechanisms to limit *Pitx2c* activity on a common set of target genes. This would include differential regulation of *Pitx2c* transcriptional levels, a mechanism that would be supported by our quantitation of *Pitx2c* mRNA levels. However, *Pitx2c* activity may also be regulated at the protein level by tight control of translation, by post-translation modification of *Pitx2c* or by the function of organ-specific co-factors that can modulate *Pitx2c* function. Further experiments

are required to distinguish between these possibilities, however, the observation of a protein-protein interaction between *Pitx2* and the pituitary-specific *pit1* support the idea that organ-specific co-factors have a role in modulating *Pitx2* function (Amendt et al., 1999).

We thank Mary Cole and Janis Smith for help with the manuscript, and R. Behringer and R. L. Johnson for comments and discussions. We thank A. Bradley, P. Soriano and R. Behringer for reagents, and A. McMahon and B. Hogan for in situ probes. Supported in part by a grant from the NIDCR (R29 DE12324) and by Basil O'Connor Starter Scholar Research Award Grant No. 5-FY97-698 from the March of Dimes to J. F. M. and the British Heart Foundation (RG/98004) to N. A. B.

REFERENCES

- Amendt, B. A., Sutherland, L. B. and Russo, A. F. (1999). Multifunctional role of the *Pitx2* homeodomain protein C-terminal tail. *Mol. Cell. Biol.* **19**, 7001-7010.
- Akawa, H., Nakamura, T., Zhadanov, A. B., Fidanza, V., Yano, T., Bullrich, F., Shimizu, M., Blechman, J., Mazo, A., Canaani, E. and Croce, C. M. (1998). Identification and characterization of the *ARPI* gene, a target for the human acute leukemia *ALL1* gene. *Proc. Natl. Acad. Sci. USA* **95**, 4573-4578.
- Bekir, N. A. and Gungor, K. (2000). Atrial septal defect with interatrial aneurysm and Axenfeld-Rieger syndrome. *Acta Ophthalmol. Scand.* **78**, 101-103.
- Bellusci, S., Furuta, Y., Rush, M. G., Henderson, R., Winnier, G. and Hogan, B. L. (1997). Involvement of Sonic hedgehog (Shh) in mouse embryonic lung growth and morphogenesis. *Development*. **124**, 53-63.
- Bellusci, S., Henderson, R., Winnier, G., Oikawa, T. and Hogan, B. L. (1996). Evidence from normal expression and targeted misexpression that bone morphogenetic protein (Bmp-4) plays a role in mouse embryonic lung morphogenesis. *Development*. **122**, 1693-1702.
- Bisgrove, B. W., Essner, J. J. and Yost, H. J. (2000). Multiple pathways in the midline regulate concordant brain, heart and gut left-right asymmetry. *Development*. **127**, 3567-3579.
- Brown, N. A. and Anderson, R. H. (1999). Symmetry and laterality in the human heart: developmental implications. In *Heart Development* (ed. R. P. Harvey and N. Rosenthal), pp. 447-462. San Diego, London, New York, Tokyo, Toronto: Academic Press.
- Brown, N. A., Hoyle, C. I., McCarthy, A. and Wolpert, L. (1989). The development of asymmetry: the sidedness of drug-induced limb abnormalities is reversed in situs inversus mice. *Development*. **107**, 637-642.
- Brown, N. A. and Wolpert, L. (1990). The development of handedness in left/right asymmetry. *Development*. **109**, 1-9.
- Campione, M., Steinbeisser, H., Schweickert, A., Deissler, K., van Bebber, F., Lowe, L. A., Nowotschin, S., Viebahn, C., Haffter, P., Kuehn, M. R. and Blum, M. (1999). The homeobox gene *Pitx2*: mediator of asymmetric left-right signaling in vertebrate heart and gut looping. *Development*. **126**, 1225-1234.
- Capdevila, J., Vogan, K. J., Tabin, C. J. and Izpisua Belmonte, J. C. (2000). Mechanisms of left-right determination in vertebrates. *Cell*. **101**, 9-21.
- Cunningham, E. T., Jr, Elliott, D., Miller, N. R., Maumenee, I. H. and Green, W. R. (1998). Familial Axenfeld-Rieger anomaly, atrial septal defect, and sensorineural hearing loss: a possible new genetic syndrome. *Arch. Ophthalmol.* **116**, 78-82.
- Echelard, Y., Epstein, D. J., St-Jacques, B., Shen, L., Mohler, J., McMahon, J. A. and McMahon, A. P. (1993). Sonic hedgehog, a member of a family of putative signaling molecules, is implicated in the regulation of CNS polarity. *Cell* **75**, 1417-1430.
- Essner, J. J., Branford, W. W., Zhang, J. and Yost, H. J. (2000). Mesendoderm and left-right brain, heart and gut development are differentially regulated by *pitx2* isoforms. *Development*. **127**, 1081-1093.
- Gage, P. J. and Camper, S. A. (1997). Pituitary homeobox 2, a novel member of the bicoid-related family of homeobox genes, is a potential regulator of anterior structure formation. *Hum. Mol. Genet.* **6**, 457-464.
- Gage, P. J., Hoonkyo, S. and Camper, S. (1999). Dosage requirement of *Pitx2* for development of multiple organs. *Development*. **126**, 4643-4651.
- Hogan, B. L. (1999). Morphogenesis. *Cell* **96**, 225-233.

- Kitamura, K., Miura, H., Miyagawa-Tomita, S., Yanazawa, M., Katoh-Fukui, Y., Suzuki, R., Ohuchi, H., Suehiro, A., Motegi, Y., Nakahara, Y., Kondo, S. and Yokoyama, M.** (1999). Mouse Pitx2 deficiency leads to anomalies of the ventral body wall, heart, extra- and periorbital mesoderm and right pulmonary isomerism. *Development*. **126**, 5749-5758.
- Lin, C. R., Kioussi, C., O'Connell, S., Briata, P., Szeto, D., Liu, F., Izpisua-Belmonte, J. C. and Rosenfeld, M. G.** (1999). Pitx2 regulates lung asymmetry, cardiac positioning and pituitary and tooth morphogenesis. *Nature* **401**, 279-282.
- Logan, M., Pagan-Westphal, S. M., Smith, D. M., Paganessi, L. and Tabin, C. J.** (1998). The transcription factor Pitx2 mediates situs-specific morphogenesis in response to left-right asymmetric signals. *Cell* **94**, 307-317.
- Lu, M. F., Pressman, C., Dyer, R., Johnson, R. L. and Martin, J. F.** (1999). Function of Rieger syndrome gene in left-right asymmetry and craniofacial development. *Nature* **401**, 276-278.
- Mammi, I., De Giorgio, P., Clementi, M. and Tenconi, R.** (1998). Cardiovascular anomaly in Rieger Syndrome: heterogeneity or contiguity? *Acta Ophthalmol. Scand.* **76**, 509-512.
- Meno, C., Shimono, A., Saijoh, Y., Yoshiro, K., Mochida, K., Ohishi, S., Noji, S., Kondoh, H. and Hamada, H.** (1998). lefty-1 is required for left-right determination as a regulator of lefty-2 and nodal. *Cell* **94**, 287-297.
- Metzger, R. J. and Krasnow, M. A.** (1999). Genetic control of branching morphogenesis. *Science* **284**, 1635-1639.
- Moore, K. L.** (1982). *The Developing Human*. Philadelphia, London, Toronto, Mexico City, Rio De Janeiro, Sydney, Tokyo: W.B. Saunders Company.
- Piedra, M. E., Icardo, J. M., Albajar, M., Rodriguez-Rey, J. C. and Ros, M. A.** (1998). Pitx2 participates in the late phase of the pathway controlling left-right asymmetry. *Cell* **94**, 319-324.
- Ryan, A. K., Blumberg, B., Rodriguez-Esteban, C., Yonei-Tamura, S., Tamura, K., Tsukui, T., de la Pena, J., Sabbagh, W., Greenwald, J., Choe, S. et al.** (1998). Pitx2 determines left-right asymmetry of internal organs in vertebrates. *Nature*. **394**, 545-551.
- Schweickert, A., Campione, M., Steinbeisser, H. and Blum, M.** (2000). Pitx2 isoforms: involvement of Pitx2c but not Pitx2a or Pitx2b in vertebrate left-right asymmetry. *Mech. Dev.* **90**, 41-51.
- Semina, E. V., Reiter, R., Leysens, N. J., Alward, W. L., Small, K. W., Datson, N. A., Siegel-Bartelt, J., Bierke-Nelson, D., Bitoun, P., Zabel, B. U., Carey, J. C. and Murray, J. C.** (1996). Cloning and characterization of a novel bicoid-related homeobox transcription factor gene, RIEG, involved in Rieger syndrome. *Nat. Genet.* **14**, 392-399.
- Supp, D. M., Witte, D. P., Potter, S. S. and Brueckner, M.** (1997). Mutation of an axonemal dynein affects left-right asymmetry in inversus viscerum mice. *Nature* **389**, 963-966.
- Uemura, H., Ho, S. Y., Devine, W. A., Kilpatrick, L. L. and Anderson, R. H.** (1995). Atrial appendages and venoatrial connections in hearts from patients with visceral heterotaxy. *Ann. Thorac. Surg.* **60**, 561-569.
- Winnier, G., Blessing, M., Labosky, P. A. and Hogan, B. L.** (1995). Bone morphogenetic protein-4 is required for mesoderm formation and patterning in the mouse. *Genes Dev.* **9**, 2105-2116.
- Yost, H. J.** (1995). Vertebrate left-right development. *Cell*. **82**, 689-692.